



LAWRENCE
LIVERMORE
NATIONAL
LABORATORY

Collisional Effects in the Ion Weibel Instability for Two Counter-Propagating Plasma Streams

D. D. Ryutov, F. R. P. Fiuza, C. M. Huntington, J.
S. Ross, H. S. Park

December 23, 2013

The Physics of Plasmas

Disclaimer

This document was prepared as an account of work sponsored by an agency of the United States government. Neither the United States government nor Lawrence Livermore National Security, LLC, nor any of their employees makes any warranty, expressed or implied, or assumes any legal liability or responsibility for the accuracy, completeness, or usefulness of any information, apparatus, product, or process disclosed, or represents that its use would not infringe privately owned rights. Reference herein to any specific commercial product, process, or service by trade name, trademark, manufacturer, or otherwise does not necessarily constitute or imply its endorsement, recommendation, or favoring by the United States government or Lawrence Livermore National Security, LLC. The views and opinions of authors expressed herein do not necessarily state or reflect those of the United States government or Lawrence Livermore National Security, LLC, and shall not be used for advertising or product endorsement purposes.

Collisional effects in the ion Weibel instability for two counter-propagating plasma streams

D. D. Ryutov, F. Fiuza, C.M. Huntington, J.S. Ross, H.-S. Park

Lawrence Livermore National Laboratory, Livermore, CA 94550

Abstract

Experiments directed towards the study of the collisionless interaction between two counter-streaming plasma flows generated by high-power lasers are designed in such a way as to make collisions between the ions of the two flows negligibly rare. This is reached by making flow velocities v as high as possible and thereby exploiting the $1/v^4$ dependence of the Rutherford cross-section. At the same time, the plasma temperature of each flow may be relatively low, so that collisional mean-free paths for the *intra-stream* particle collisions may be much smaller than the characteristic spatial scale of the unstable modes required for the shock formation. The corresponding effects are studied in this paper for the case of the ion Weibel (filamentation) instability. Dispersion relations for the case of strong intra-stream collisions are derived. It is shown that the growth-rates become significantly smaller than those stemming from a collisionless model. The underlying physics is mostly related to the increase of the electron stabilizing term. Additional effects are an increased “stiffness” of the collisional ion gas and the ion viscous dissipation. A parameter domain where collisions are important is identified.

I. INTRODUCTION

Electromagnetic instabilities of two counter-propagating plasma flows [1, 2] are an interesting example of the plasma physics effects important for astrophysics. In particular, these instabilities can be responsible for generation of magnetic field in initially un-magnetized plasmas, formation of collisionless shocks, and particle acceleration (see, e.g., Refs. 3-8 and references therein). Significant attention has been drawn by the possibility of studying these effects in the plasma flows obtained by the plasma ablation from the properly-oriented targets irradiated by intense lasers (e.g., [9-13]). The interpenetrating flows are expected to generate the ion Weibel instability leading to formation of current filaments aligned with the flow. The magnetic field generated by these currents scatter the charged particles and may lead to the formation of collisionless shocks and to particle acceleration.

The ideal plasma for investigating collisionless shocks in counter-streaming flows would be a hydrogen plasma. However, for practical reasons the targets (and, therefore, plasma jets) are made not of hydrogen, but of materials like beryllium, carbon, or polymers. This leads to an increase of the ion-ion collision cross-sections, which scale as the ion charge Z to the fourth power. Still, the conditions in these experiments can be adjusted in such a way as to make collisions between the ions of the two jets (inter-jet collisions) negligible. For the typical carbon ion densities in the flows of order of 10^{18} cm^{-3} and the flow velocities approaching 10^8 cm/s the carbon-carbon collisional mean-free-path (m.f.p.) is on the order of 10 cm, whereas the size of the interaction zone of the two streams is a few millimeters [9-13].

On the other hand, the collisions between the ions in each jet may be important (see, e.g., [10, 14]). This is a consequence of the fact that the jets, by design, have high Mach numbers, so that the plasma temperature T is much lower than the ion directional energy, whereas the Coulomb collision cross-section scales as $1/T^2$. In a case where the ion temperature is 100 times lower than their directional energy, the mean-free path for the intra-jet ion collisions may become very short.

In this article we study the effect of intra-jet collisions on the linear stage of the Weibel instability and identify regimes where these collisions significantly affect the instability. For realistic plasma parameters, not only ion-ion, but also electron-ion collisions may play significant role. Additionally, the presence of hydrogen or deuterium in the plasma (as is the case for plastic targets) may have a strong stabilizing effect. Our overall conclusion is that, for the typical densities of the experiments of the type [9], the collisional effects on the Weibel instability become decisively unimportant for the plasma temperatures in each stream exceeding 1 keV, as is the case in, e.g., Ref. 10. At lower temperatures one must be careful in comparing experimental results with the results of collisionless simulations.

Table 1 The collisionality characteristics of two interpenetrating streams*

| 1 | 2 | 3 | 4 | 5 | 6 | 7 | 8 | 9 |
|-------------------------|----------------------|-----------------------|----------------------|----------------------|----------------------|--------------------|----------------------------|--------------------------------|
| | $l_{ZZ},$ μm | ν_{ZZ}, s^{-1} | $l_{eZ},$ μm | ν_{eZ}, s^{-1} | $l_{HZ},$ μm | ν_{HZ}, s^{-1} | c/ω_{pi} μm | $(v/c)\omega_{pi}$ s^{-1} |
| $T_e=T_i=0.25$ keV | 0.85 | 7.5×10^{10} | 10.9 | 8.7×10^{11} | 22 | 2×10^{10} | 60 | 1.2×10^{10} |
| $T_e=T_i=0.50$ keV | 3.4 | 2.65×10^{10} | 44 | 3.7×10^{11} | 88 | 7×10^9 | 60 | 1.2×10^{10} |
| $T_e=T_i=1.00$ keV | 13.6 | 9.4×10^9 | 175 | 1.1×10^{11} | 350 | 2.5×10^9 | 60 | 1.2×10^{10} |

* Velocity of each stream is $v=8 \times 10^7$ cm/s, kinetic energy of the carbon ions in each stream is $W_Z=40$ keV, total electron density is $n_e=2 \times 10^{19}$ cm⁻³. The ion plasma frequency ω_{pi} in this table is evaluated for a purely carbon plasma, and the effect of the hydrogen admixture on the carbon density at a given total electron density is neglected ($\sim 20\%$ changes are discussed in the corresponding parts of this article). Notation: l_{ZZ} and ν_{ZZ} are carbon-carbon mean-free path and carbon-carbon collision frequency for the intra-stream collisions; l_{eZ} (l_{HZ}) and ν_{eZ} (ν_{HZ}) are the corresponding quantities for the electron-carbon (hydrogen-carbon) collisions.

To illustrate relative role of various types of collisions, we summarize the mean-free-paths and collision frequencies for a range of plasma temperatures in Table 1. The last two columns contain the characteristic wave-number of the ion Weibel instability,

$$k = \omega_{pi} / c, \quad (1)$$

where ω_{pi} is the ion plasma frequency and c is the speed of light, and the characteristic growth rate

$$\Gamma = \omega_{pi} \frac{v}{c}, \quad (2)$$

where v is the flow velocity. In order for a certain type of collisions to be unimportant, the corresponding mean-free path has to be longer than $1/k$ and the corresponding collision rate has to be smaller than the characteristic growth rate Γ . However, with regard to the growth rate, one must remember that the actual growth rate in a number of cases is almost an order of magnitude lower than its “characteristic” value (see below).

The ion-ion collision frequencies given in Table 1 are evaluated based on Eq. (2.5i) in Ref. 15. The electron-ion collision frequencies are evaluated based on Eq. (2.5e) in Ref. 15; the ion density in this case is a total ion density of two streams, as the electron thermal velocity is much higher than u in all cases, and the electron-ion scattering frequency can be evaluated under the assumption that the ions have no velocity spread. The Coulomb logarithm was taken to be equal to 10 in all cases. The mean-free paths are evaluated by dividing the thermal velocity - defined by $v_T = \sqrt{2T/m}$, with the mass and temperature of the species in question - by the corresponding collision frequency.

We show below that the actual instability growth rate is much smaller than the reference value (column 9 in Table 1), so, actually, a relatively low collision frequency for the hydrogen-carbon collisions (column 7) remains much higher than the growth rate. In this regard, the hydrogen is collisional for the parameters in first two rows of Table 1. Some apparent difference between the electron and hydrogen m.f.p. at the same electron and ion temperatures is related to the fact that the electrons scatter on the ions of both flows. With increasing electron temperature, electrons become collisionless for the temperatures exceeding 0.5 keV.

We consider the case of symmetric jets, with identical parameters, propagating in the opposite directions. The electrons, due to their very high thermal velocity, behave as a single component, into which both ion streams are immersed. For the symmetric jets, this component in the unperturbed state is at rest. Each ion stream in a highly collisional regime is to be described by hydrodynamical equations and is characterized by the temperature, density and directed velocity; hydrodynamic viscosity has to be included to account for the internal friction in the ion flow. The same approach will be applied to the electron component when it is collisional.

The paper is organized as follows. In Section II, we specify the geometry used in the stability analysis and write down basic equations. In Sec. III, we study the ion dynamics for the case of one ion species. In Sec. IV, we do a similar analysis for the electron component. Having found the electron and ion current perturbations and substituting them to the Maxwell equations, we find a dispersion relation, which is derived and analyzed in Sec. V. In Sec. VI we consider an effect of the light ion admixture and find that it can lead to a strong decrease of the growth rate due to increased compressional “stiffness” of the ion population and higher viscosity of the mixture [16, 17]. In Sec. VII we summarize the results.

II. FORMULATION OF THE PROBLEM

We assume a uniform and stationary unperturbed state and consider the perturbations depending on space and time as $\exp(\Gamma t + i\mathbf{k} \cdot \mathbf{r})$, where Γ is a complex

growth rate and k is the wave vector). We assume that the streams are flowing along the axis z , and the wave vector is perpendicular to this axis. We orient the coordinate frame so as to make axis x parallel to the wave vector. In other words, wave vector has only x component. This is a canonical setting for the Weibel instability (e.g., [1-2], [18-19]). In this geometry, the perturbed magnetic field will have only the y component (δB_y) and the perturbed electric field only the z component (δE_z). The appropriate components of the Maxwell equations then yield:

$$ik_x \delta B_y = \frac{4\pi}{c} \delta j_z \quad (3)$$

and

$$ik_x \delta E_z = \Gamma \delta B_y . \quad (4)$$

For symmetric streams, the unstable modes are found to be the modes of a pure growth, with a real Γ .

In the further sections, we will express the current perturbation in terms of δB_y and δE_z , and thereby close the system of equations (3), (4). The solubility condition for this linear homogeneous set of equations then yields the dispersion relation.

III. THE ION RESPONSE

Consider the ion stream moving in the positive direction of the axis z . We find its contribution to the current perturbation and then find the contribution of the oppositely directed stream just by changing a few signs in the first expression. We consider here a plasma with a single ion species. A generalization to a plasma consisting of both heavy and light species is described in Sec. VI.

The perturbed hydrodynamic equations for the ions of a stream propagating in the positive z direction are:

$$\Gamma \delta v_x = -ik_x \frac{\delta p_i}{Am_p n_i} - \frac{Zev \delta B_y}{Am_p c} - \eta_b k_x^2 \delta v_x , \quad (5)$$

$$\Gamma \delta v_z = \frac{Ze \delta E_z}{Am_p} - \eta_s k_x^2 \delta v_z , \quad (6)$$

where subscripts “b” and “s” designate the bulk and shear viscosities that differ by a factor of order one (see below). The ion density n_i relates here to a single stream. The total ion density is

$$2n_i = n_e / Z \quad (7)$$

where n_e is the total electron density. The pressure perturbation is related to the density perturbation by

$$\delta p_i = \frac{5}{3} T_i \delta n_i . \quad (8)$$

Given a strong ion collisionality, we use a collisional ion adiabat. The ion density perturbation is related to δv_{ix} via the continuity equation:

$$\Gamma \delta n_i + ik_x n_i \delta v_{ix} = 0 \quad (9)$$

We emphasize that these equations are related to a single ion stream.

For the stream moving in the opposite direction, the density perturbation and the x component of the velocity perturbation have the opposite sign compared to the ion stream moving in the forward direction; the z component of the velocity perturbation has the same sign. This circumstance can be seen from Eqs. (5-6) and (9) upon the change of the sign of the unperturbed velocity.

The ion current perturbation is:

$$\delta j_{zi} = Ze(n_i \delta v_{z_i} + v \delta n_i) + \dots \quad (10)$$

where the dots mean a contribution of the opposite stream. The unperturbed velocity v for the second stream is negative and, as mentioned, the density perturbation in it has an opposite sign with respect to the density perturbation in the first stream, whereas the z component of the velocity perturbation has the same sign. This means that the total perturbation of the ion current is just twice the current perturbation of the first stream:

$$\delta j_{zi} = 2Ze(n_i \delta v_{z_i} + v \delta n_i) = en_e \left(\delta v_{z_i} + v \frac{\delta n_i}{n_i} \right) \quad (11)$$

The total ion density perturbation is zero. Using Eqs. (5), (6), (8), (9) and (11), one can express the ion current perturbation in terms of the magnetic field perturbation:

$$\delta j_{zi} = i \delta B_y \frac{\omega_{pi}^2}{4\pi k_x c} \left[-\frac{\Gamma}{\Gamma + \eta_s k_x^2} + \frac{k_x^2 v^2}{\Gamma(\Gamma + \eta_b k_x^2) + k_x^2 s^2} \right], \quad (12)$$

where $s = \sqrt{(5/3)(T_i / Am_p)}$ is the ion sound speed, and $\omega_{pi}^2 = \frac{4\pi n_e e^2 Z}{m_p A}$ is the ion plasma

frequency. The drive for the filamentation instability is associated with the last term in the square bracket and is proportional to the square of the velocity of the counterstreaming jets.

IV. THE ELECTRON RESPONSE

Due to a high electron mobility, electrons play a stabilizing role by partially cancelling the ion current and thereby disrupting the feedback loop. For the electron temperature of 250 eV, the electron mean free path in a carbon plasma with the reference parameters of Table 1 is $\lambda_{ei} \sim 10^{-3} cm$, and the electron-ion collision frequency is $\nu_{ei} \sim 10^{12} s^{-1}$. In other words, the electrons are also highly collisional, and their response can be found by using a description via the electron hydrodynamic equations [15]. In doing so, we note that the electron thermal velocity even at a relatively low temperature of 100 eV is still much higher than the velocity of the ion streams. So, electron collisions with the ions can be considered as scattering from ions having a zero velocity spread. Then, the z -component of the electron momentum equation can be written as:

$$(\Gamma + k_x^2 \eta_{se}) \delta v_{ze} = -\frac{e}{m} \delta E_z - \nu_{ei} \left(\delta v_{ze} - \frac{\delta j_{zi}}{2Zn_z} \right), \quad (13)$$

where η_{se} is electron shear viscosity. The term $\delta j_{zi} / 2n_z$ represents an average (between two streams) perturbation of the z -component of the ion velocity. We recall that n_z is the ion density per stream. So, there are two relaxation terms in Eq. (13): the electron-ion friction (the term proportional to ν_{ei} in the right-hand side), and the viscous term in the

left-hand side. [Note that we neglected the friction force in the ion momentum equation because of a low electron-to-ion mass ratio.]

The viscous term causes relaxation of the sheared electron velocity. When the plasma parameters approach the collisionless limit, this term is replaced by the relaxation of the sheared velocity by the electron thermal motion. It is accounted for in the collisionless version of the electron response by the term $\sim k_x v_{Te}$ [2, 18], which appears instead of the viscous term.

As the ion density perturbation is absent, and the plasma is quasineutral, the electron density perturbation is also zero. We also note that, since the electron fluid was at rest in the unperturbed state, there is no Lorenz force acting on the electrons in the linear approximation.

By noting that

$$\delta j_z = -en_e \delta v_{ze} + \delta j_{zi}, \quad (14)$$

one finds from Eq. (13) that the electron current perturbation is given by:

$$\delta j_{ze} = i\delta B_y \frac{\omega_{pe}^2}{4\pi k_x c} \frac{\Gamma + \frac{k_x^2 c^2}{\Gamma + k_x^2 \eta_{se}}}{\Gamma + k_x^2 \eta_{se}} \quad (15)$$

V. THE DISPERSION RELATION

A. Collisional case

By summing up Eqs. (12) and (15), and using Eq. (3), we arrive at the dispersion relation for the Weibel-like instability:

$$\frac{k_x^2 c^2}{\omega_{pi}^2} = -\frac{\omega_{pe}^2}{\omega_{pi}^2} \frac{\Gamma + \frac{k_x^2 c^2}{\Gamma + k_x^2 \eta_{se}}}{\Gamma + k_x^2 \eta_{se}} - \frac{\Gamma}{\Gamma + \eta_s k_x^2} + \frac{k_x^2 v^2}{\Gamma(\Gamma + \eta_b k_x^2) + k_x^2 s^2} \quad (16)$$

The first two terms (those with the “minus” sign in front of them) on the right-hand side are stabilizing terms. The first of them is related to the electron current that partially neutralizes the ion current in the z direction. The second comes from the term $\sim n_i \delta v_{iz}$ in Eqs. (10), (11) and corresponds to the analogous ion contribution to the current neutralization. To establish connection to the standard Weibel instability, we drop these stabilizing terms in the dispersion relation; we drop also the viscous term. This yields:

$$\Gamma^2 = \frac{k_x^2 v^2}{1 + \frac{k_x^2 c^2}{\omega_{pi}^2}} - k_x^2 s^2 \quad (17)$$

For $v \gg s$ the growth-rate of order of (2) is reached for k determined by Eq. (1).

Consider now the general dispersion relation (16). Normalizing Γ to $(v/c)\omega_{pi}$ and k_x to ω_{pi}/c , one can present the dispersion relation in the dimensionless form:

$$k^2 + \mu \frac{\Gamma + k^2 R}{\Gamma + k^2 V_{se}} + \frac{\Gamma}{\Gamma + V_s k^2} = \frac{k^2}{\Gamma(\Gamma + V_b k^2) + S k^2}, \quad (18)$$

where we have introduced five dimensionless parameters:

$$\mu = \frac{Am_p}{Zm_e}; R = \frac{\omega_{pi}c}{4\pi v\sigma}; V_{se} = \frac{\eta_{se}\omega_{pi}}{vc}; V_{b,s} = \frac{\eta_{b,s}\omega_{pi}}{vc}; S = \frac{s^2}{v^2}, \quad (19)$$

which characterize the mass ratio (μ), the resistive effects (R), the viscous effects (V_{se} , V_s and V_b), and the ion sound speed (S). For the dimensionless wave number we use notation “ k ”.

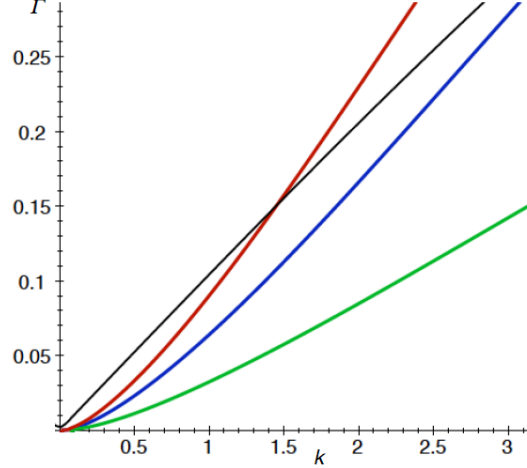


Fig 1. The dimensionless growth rate vs the dimensionless wave number for $T_e = T_i = 0.15$ keV (green line) $T_e = T_i = 0.25$ keV (blue line), and $T_e = T_i = 0.35$ keV (red line). Note that the grow rates at the “characteristic” wave number (1) is 10-30 times lower than the “characteristic” growth rate (2). The black curve corresponds to the collisionless dispersion relation for $T_e = T_i = 0.15$ keV and is presented here merely for reference (as the collisionality is actually high). This reference line lies noticeably above the green line.

To make a parameter scan of the instability at various values of T_e and T_i , we present the values of all the dimensionless parameters (19) as functions of the temperatures for the fixed values of the electron density and ion directed velocity corresponding to Table 1: $n_e = 2 \times 10^{19} \text{ cm}^{-3}$ and $v = 8 \times 10^7 \text{ cm/s}$. Using Ref. 15, we find:

$$R = \frac{1.06 \times 10^{-3}}{[T_e(\text{keV})]^{3/2}}; V_s = 1.75 \times 10^{-2} [T_i(\text{keV})]^{5/2}; V_b = 2.53 \times 10^{-2} [T_i(\text{keV})]^{5/2} \quad (20)$$

$$V_{se} = 64 [T_e(\text{keV})]^{5/2}; S = 1.4 \times 10^{-2} T_i(\text{keV})$$

If a dimensionless parameter of the set (19) is very small, this means that the corresponding effect does not influence the instability. For the parameter domain of the experiments of the type [9, 10], the resistive effects are small and the term proportional to R can be neglected. Conversely, the term related to electron viscosity can be important. The other effects are relatively weak but may lead to quantitative corrections of order of 10-20%. However, their role may increase substantially for the plasmas containing a significant hydrogen component (Sec. VI).

Figure 1 shows normalized growth rates vs normalized wave numbers for several temperatures. We concentrate at the small-to-moderate values of $k < 2$, as for the higher k 's the collisionality constraint may be violated for the electrons and, eventually, for the ions. A broader analysis accounting for this possibility is presented in Sec. VC. One sees that for the reference wave number (1) the growth rate is at least an order of magnitude

smaller than its reference value (2). One sees also that the growth rate increases with the temperature. This is mostly due to the higher electron viscosity at higher temperatures.

B. Comparison to a collisionless case

The derivation of the dispersion relation for the collisionless case can be found in Ref. 2. The result can be presented as:

$$\frac{k_x^2 c^2}{\omega_{pi}^2} = -\frac{\omega_{pe}^2}{1 + \frac{|k_x| \sqrt{2T_e}}{\Gamma} \sqrt{\pi m_e}} - G_1 \left(\frac{\Gamma^2 A m_p}{2k_x^2 T_z} \right) + \frac{k_x^2 v^2}{\Gamma^2} G_2 \left(\frac{\Gamma^2 A m_p}{2k_x^2 T_z} \right) \quad (21)$$

where

$$G_1(y) = \frac{1}{\sqrt{\pi}} \int_{-\infty}^{+\infty} \frac{y e^{-x^2}}{x^2 + y} dx; \quad G_2(y) = \frac{2y}{\sqrt{\pi}} \int_{-\infty}^{+\infty} \frac{x^2 e^{-x^2}}{x^2 + y} dx. \quad (22)$$

For a quick orientation, we will use the following interpolations for the functions G_1, G_2 :

$$G_1(y) = \frac{1}{1 + \frac{1}{\sqrt{\pi y}}}; \quad G_2(y) = \frac{2y}{1 + 2y}. \quad (23)$$

These interpolations correctly capture the asymptotic behavior of these functions at both large and small y and are sufficiently accurate for the intermediate values of y .

With this substitution made, dispersion relation (21) acquires the structure quite similar to Eq. (18):

$$k^2 + \mu \frac{\Gamma}{\Gamma + U_e |k_x|} + \frac{\Gamma}{\Gamma + U_i |k_x|} = \frac{k^2}{(3S/5)k^2 + \Gamma^2} \quad (24)$$

where

$$U_{e,i} = \frac{v_{Te,i}}{v \sqrt{\pi}} \quad (25)$$

For our “standard” value of $v=8 \times 10^7$ cm/s, one has: $U_e = 12 \sqrt{T_e (keV)} > 1$, whereas U_i is usually negligibly small. The terms containing U in the denominator are responsible for damping of the z component of the current by the perpendicular (along x) thermal motion of the electrons and ions. This effect is particularly important in the electron contribution that contains a very large factor μ .

Comparing Eqs. (18) and (24), one finds the following main differences: 1) The electron stabilizing term in the collisional equation (18) is suppressed by the electron viscosity, not by the free thermal streaming. This difference is key for the explanation of the lower growth rates in the collisional case: the viscous suppression of the sheared electron current is much weaker at lower temperatures than the suppression by unimpeded thermal motion in the x direction. 2) The stabilizing effect of the ion pressure (the terms proportional to S in both equations) is weaker in the collisionless case due to the factor of $3/5$ in Eq. (24) that reflects a higher “stiffness” of the collisional gas. 3) Stabilizing viscous terms (those proportional to V_s and V_b) are absent in the collisionless case.

The difference in the structure of the stabilizing ion terms is unimportant, because these terms are small in both cases compared to the electron stabilizing terms.

The solution of the dispersion relation (24) is shown as a black line in Fig. 1, for reference. As anticipated, the difference between the two models is strongest at longer wavelengths. We will see in Sec. VI that the difference becomes much stronger for the CH₂ case.

C. Generalized dispersion relation covering both collisional and collisionless electrons

In this section we will present a dispersion relation that covers both collisional and collisionless effects. We note that the viscosity of a pure high-Z plasma (in particular, carbon plasma) is quite small, and the viscous term in Eq. (18) can be neglected. The second term in the denominator of the ion stabilization term is also small, and we neglect it. In this approximation, the ion-stabilizing term in both cases becomes merely one. As mentioned above, the magnetic diffusivity term in the numerator of the electron stabilizing term is small, and we neglect it.

In the remaining expression for the electron stabilizing term we use an interpolation between the large and small electron collisionality. To do that, we suggest presenting the denominator in the form: $\Gamma + \Gamma_e(|k_x|)$, where

$$\Gamma_e(|k_x|) = \frac{(V_e k_x^2)(U_{se} |k_x|)}{\sqrt{(V_e k_x^2)^2 + (U_{se} |k_x|)^2}} \quad (26)$$

where V_e and U_e are defined by Eqs. (19) and (25), respectively. For a given wave number, the viscous term dominates at a lower temperature, whereas the streaming effect dominates at higher temperatures.

In a similar fashion, we use interpolation for the compressibility term in the denominator of the right-hand-side of Eqs. (18), (24). In these terms, the transition from collisional description to a collisionless one occurs for $|k_x| l_{ZZ} = 1$. To describe the transition from the term Sk^2 in the collisional case (18) to the term $(3/5)Sk^2$ in the collisionless case (24), we use an interpolation function $F(k)$ defined as

$$F(k) = 1 - \frac{2}{5} \frac{C |k|}{\sqrt{1 + C^2 k^2}}, \quad (27)$$

where the dimensionless parameter C (“collisionality”) is

$$C = l_{ZZ} \omega_{pi} / c, \quad (28)$$

and k in this equation is a dimensionless wave number normalized to ω_{pi} / c . For the basic parameters (n_e and v) of Table 1, the numerical value of the coefficient C for carbon is:

$$C = 0.23 T_i^2 (keV) \quad (29)$$

The function F is equal to 1 at a high collisionality (small Ck) and $3/5$ at a low collisionality (large Ck), so that the unified expression for the r.h.s. of Eq. (18) and Eq. (24) becomes:

$$\frac{k^2}{\Gamma^2 + SF(k)k^2} \quad (30)$$

This preparatory work leads to the following dispersion relation that unifies a collisional and collisionless case for a purely high-Z plasma:

$$k^2 + 1 + \frac{\mu\Gamma}{\Gamma + \Gamma_e(k)} = \frac{k^2}{\Gamma^2 + F(k)Sk^2} \quad (31)$$

This equation is accurate to within a few percent for both collisional and collisionless domains and provides a smooth connection between the two. The dispersion curves for carbon are illustrated by Fig. 2 for the basic parameters (n_e and v) as in Table 1.

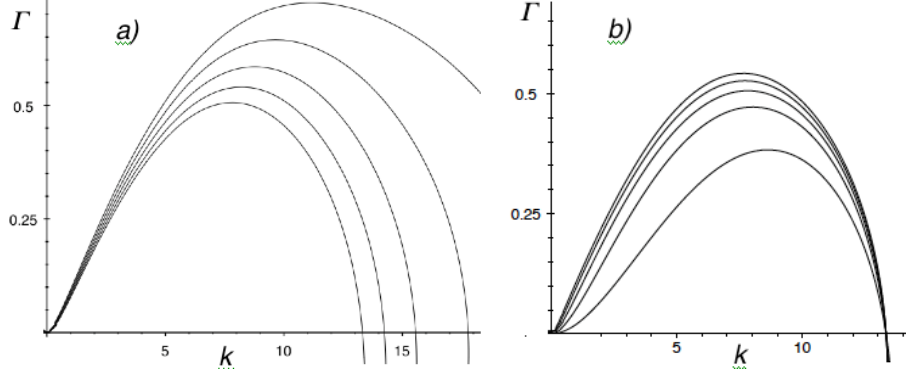


Fig. 2 A broad scan over the wave numbers and temperatures for a unified model: a) Scan over the ion temperatures for $T_e=0.35$ keV; the ion temperatures are $T_i=0.15$ keV , 0.25 keV , 0.35 keV , 0.45 keV and 0.55 keV from the upper to the lower curve; b) Scan over the electron temperatures for $T_i=0.55$ keV; the electron temperatures are $T_e=0.15$ keV , 0.25 keV , 0.35 keV , 0.45 keV and 0.55 keV from the lower to the upper curve. Note that the maximum growth rate is reached for k about 10 times higher than the reference value (1) and is roughly 2 times smaller than the reference value (2).

VI. EFFECT OF THE LIGHT ION ADMIXTURE

In this section we consider the effect of a light-ion component present in both flows. One meets such a situation when both targets are made of a plastic, e.g. of CH_2 . In the regimes where both ion components are collisional (within each jet, Table 1), the main effect caused by the presence of the hydrogen (or deuterium) is related to a significant increase of the viscosity. As noted in Ref. [16], the larger mean-free path of the $Z=1$ ions makes their contribution to viscosity very significant. In particular, the viscosity of CH_2 plasma is roughly 20 times higher than the viscosity of a purely carbon plasma [16, 17]. Additional stabilization arises from an increased “stiffness” of the ion component, where there are now two more ions contributing to the ion pressure.

In plasmas with multiple ion species the number of possible collisionality regimes becomes too large to be treated in a comprehensive way. In this study, we focus on the regime of the modest-to-low temperatures (below 0.5 keV) and modest normalized wave numbers ($k < 3$), where all the species are collisional. We leave a more detailed study of the regimes of intermediate collisionalities for future work.

When both ion components are strongly coupled, as is the case for the first two rows of Table 1, the ions in each stream behave as a single gas with a pressure

$$p_i = n_z T_i (1 + \alpha), \quad (32)$$

where n_z is a heavy ion density per stream and α is a number of hydrogen ions per one heavy (Z) ion. The ion density per stream is

$$\rho_i = m_p n_z (A_Z + \alpha A_H), \quad (33)$$

where A_H is an atomic mass of a light ion: we allow for it to be 1, 2, or 3 to account for the possible use of a deuterated or tritiated targets. The ion sound speed under such conditions is

$$s^2 = \frac{5}{3} \frac{T_i}{m_p} \frac{1 + \alpha}{A_Z + \alpha A_H} \quad (34)$$

For the CH_2 plasma, $s^2 = (5/14)(T_i/m_p)$.

The number of electrons (in two streams) is

$$n_e = 2n_z(Z + \alpha) \quad (35)$$

and the ion plasma frequency is

$$\omega_{pi}^2 = \omega_{pe}^2 \frac{m_e}{m_p} \frac{Z + \alpha}{A_Z + \alpha A_H}. \quad (36)$$

For the CH_2 plasma, the ratio $\omega_{pe}^2/\omega_{pi}^2$ that enters the dispersion relation is $(7/4)(m_p/m_e)$ and is slightly lower than for the pure carbon plasma. The presence of hydrogen, causes a reduction of the number of carbon ions per one electron (by 25% in case of CH_2). This leads to a slight decrease of the collisionality, which is almost entirely determined by the heavy ions.

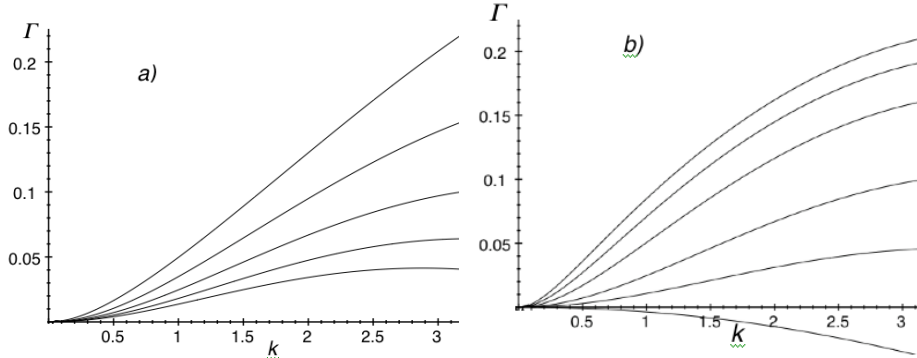


Fig. 3 The growth rates for the CH_2 plasma: a) $T_e=0.25$ keV and $T_i=0.15$ keV, 0.25 keV, 0.35 keV, 0.45 keV, 0.55 keV (from the upper to the lower curve); in all cases the growth-rate for the characteristic wave number of $k=1$ is less than $1/20$ of the normalized growth rate. b) $T_i=0.35$ keV and $T_e=0.15$ keV, 0.20 keV, 0.25 keV, 0.35 keV, 0.45 keV and 0.55 keV (from the lower to the upper curve). For $T_e=0.15$ keV the mode is stable; in other cases, the growth rate for $k=1$ is below $\sim 1/15$ of the reference growth rate (2).

As mentioned at the beginning of this section, the most dramatic change occurs in the ion viscosity that increases by a factor of 20-30 compared to the pure carbon case. Using the simple expression presented in Ref. [16] one finds that, for the CH_2 plasma (of a given electron density) the increase is approximately a factor of 25.

We are now prepared to assess the growth rates for the CH_2 plasmas. The dimensionless parameter μ is now 3220, and the other dimensionless parameters entering Eq. (18) have to be changed in the following way: R and V_{se} multiplied by $3/4$; V_{si} and V_{bi} multiplied by 25; S increased by 2.6. The results are presented in Fig. 3.

As anticipated, the enhanced viscosity leads to a further decrease of the growth rates compared to the case of a pure carbon plasma, especially at higher ion temperatures. Taking these effects together, the presence of the light component makes the instability significantly weaker than it was for a pure carbon. Hotter electrons cause some increase in the growth rates.

Numerically, the growth rates become quite low. For the plasma parameters of Table 1 and the wave number equal to the reference wave number (1), the growth rate is in the range of $(2-3)10^8 \text{ s}^{-1}$. For the typical duration of the interaction phase of two streams of 2-3 ns, this is insufficient to give rise to well-developed filaments. Even for three times higher wave-numbers the growth rate is still quite small. Note that the collisionality effects are particularly strong in the presence of a light species.

VII DISCUSSION

The changes introduced by collisional effects in the filamentation instability of two colliding plasma jets can be quite significant. They occur predominantly due to the effect of electron-ion collisions on the electron contribution: the electron stabilization becomes much stronger due to the suppression of the free electron streaming in the transverse direction. The other changes caused by the collisionality are the increased “stiffness” of the ion gas and the appearance of the ion viscosity. The last two effects are particularly important for the streams containing hydrogen or its isotopes. For the wave numbers below, roughly, $3(\omega_{pi}/c)$, the growth rates become significantly smaller than those predicted by the collisionless model. At higher wave numbers (shorter wavelengths) the collisional effects become less important albeit non-negligible.

There are interesting intermediate regimes where the high-Z ions are strongly collisional (within each jet), but electron collisions and proton collisions with these heavy ions become weak. This occurs due to the different dependence of these collisions on the heavy ion Z: the Z-Z collision cross section scales as Z^4 , while the e-Z and H-Z cross-sections scale as Z^2 . Derivation of the dispersion relations for these intermediate regimes is a subject of future studies.

In order to reach fully collisionless regimes, one can use two approaches, separately or in parallel. The first would be to increase both the directed energy and the temperature of the plasma streams, so that the intra-jet collisions become less significant, while the Mach number would remain high, allowing for a clearer identification of collisionless shock formation. The other approach would be to use streams made of lighter materials, like beryllium or lithium.

ACKNOWLEDGMENT

This work was performed under the Auspices of the U.S. Department of Energy by Lawrence Livermore National Security, LLC, Lawrence Livermore National Laboratory, under Contract DE-AC52-07NA27344.

References

1. E.S. Weibel. “Spontaneously growing transverse waves in a plasma due to an anisotropic velocity distribution.” *Phys. Rev. Letters*, **2**, 83 (1959).
2. Ronald C. Davidson, David A. Hammer, Irving Haber, and Carl E. Wagner. “Nonlinear development of electromagnetic instabilities in anisotropic plasmas.” *Physics of Fluids*, **15**(2), 317, 1972.
3. R. M. Kulsrud, R. Cen, J. P. Ostriker, and D. Ryu “The protogalactic origin for cosmic magnetic fields.” *Astrophys. J.*, **480**, 481 (1997)
4. A. Gruzinov and E. Waxman. “Gamma-ray burst afterglow: Polarization and analytic light curves.” *Astrophys. J.*, **511**, 852–861, 1999.
5. Mikhail V. Medvedev and Abraham Loeb. “Generation of magnetic fields in the relativistic shock of gamma-ray burst sources.” *The Astrophysical Journal*, **526**(2):697, 1999.
6. A. Spitkovsky. “On the structure of relativistic collisionless shocks in electron-ion plasmas”. *The Astrophysical Journal Letters*, **673**(1):L39, 2008;
7. Tsunehiko N. Kato and Hideaki Takabe. “Nonrelativistic collisionless shocks in unmagnetized electron-ion plasmas.” *The Astrophysical Journal Letters*, **681**(2):L93, 2008.
8. S. F. Martins, R. A. Fonseca, L. O. Silva, and W. B. Mori. “Ion dynamics and acceleration in relativistic shocks”. *The Astrophysical Journal Letters*, **695**(2):L189, 2009;
9. H.-S. Park, D.D. Ryutov, J.S. Ross, N.L. Kugland, S.H. Glenzer, C. Plechaty, S.M. Pollaine, B.A. Remington, A. Spitkovsky, L. Gargate, G. Gregori, A. Bell, C. Murphy, Y. Sakawa, Y. Kuramitsu, T. Morita, H. Takabe, D.H. Froula, G. Fiksel, Miniati, M. Koenig, A. Ravasio, A. Pelka, E. Liang, N. Woolsey, C.C. Kuranz, R.P. Drake, and M.J. Grosskopf. “Studying astrophysical collisionless shocks with counterstreaming plasmas from high power lasers,” *High Energy Density Physics* **8**, 38 (2012).
10. J.S. Ross, S.H. Glenzer, P. Amendt, R. Berger, L. Divol, N.L. Kugland, O.L. Landen, C. Plechaty, B. Remington, D. Ryutov, W. Rozmus, D.H. Froula, G. Fiksel, C. Sorce, Y. Kuramitsu, T. Morita, Y. Sakawa, H. Takabe, R.P. Drake, M. Grosskopf, C. Kuranz, G. Gregori, J. Meinecke, C.D. Murphy, M. Koenig, A. Pelka, A. Ravasio, T. Vinci, E. Liang, R. Presura, A. Spitkovsky, F. Miniati, and H.-S. Park. “Characterizing counter-streaming interpenetrating plasmas relevant to astrophysical collisionless shocks” *Phys. Plasmas*, **19**, 056501 (2012).
11. N.L. Kugland, S. Ross, Po-Yu Chang, R. P. Drake, G. Fiksel, D. Froula, S. H. Glenzer, G. Gregori, M.J. Grosskopf, C. M. Huntington, M. Koenig, Y. Kuramitsu, C. C. Kuranz, M. C. Levy, Edison Liang, David Martinez, J. Meinecke, Francesco Miniati, Taichi Morita, A. Pelka, C. Plechaty, Radu Presura, Alessandra Ravasio, Bruce A. Remington, Brian Reville, D. D. Ryutov, Y. Sakawa, A. Spitkovsky, Hideaki Takabe, Hye-Sook Park. “Visualizing electromagnetic fields in laser-produced counter-streaming plasma experiments for collisionless shock laboratory astrophysics.” *Phys. Plasmas*, **20**, 056313, May 2013.

12. C. M. Huntington, F. Fiuza, J. S. Ross, A. B. Zylstra, R. P. Drake, D. H. Froula, G. Gregori, N. L. Kugland, C. C. Kuranz, M. C. Levy, C. K. Li, J. Meinecke, T. Morita, R. Petrasso, C. Plechaty, B. A. Remington, D. D. Ryutov, Y. Sakawa, A. Spitkovsky, H. Takabe, H.-S. Park. "Observation of magnetic field generation via the Weibel instability in interpenetrating plasma flows." arXiv:1310.3337, October 12, 2013.
13. W. Fox, G. Fiksel, A. Bhattacharjee, P.-Y. Chang, K. Germaschewski, S. X. Hu, and P. M. Nilson "Filamentation Instability of Counterstreaming Laser-Driven Plasmas." PRL **111**, 225002 (2013)
14. D.D. Ryutov, N. L. Kugland, H.-S. Park, C. Plechaty, B.A. Remington, J. S. Ross. "Intra-Jet Shocks in Two Counter-Streaming, Weakly Collisional Plasma Jets." Phys. Plasmas, **19**, 074501, July 2012, LLNL-JRNL-550992.
15. S.I. Braginski, "Transport Processes in a Plasma," In: Reviews of Plasma Physics, M.A. Leontovich, Ed. Consultants Bureau, New York, 1965.
16. D.D. Ryutov. "Rayleigh-Taylor Instability in a Finely Structured Medium". Physics of Plasmas, **3**, 4336 (1996).
17. M. Dorf, in preparation (2014).
18. R.L. Berger, J.R. Albritton, C.J. Randall, E.A. Williams, W.L. Kruer, A.B. Langdon, C.J. Hanna. "Stopping and thermalization of interpenetrating plasma streams" Phys. Fluids, **B3**, 3 (1991).
19. R.P. Drake and G. Gregori. "Design considerations for unmagnetized collisionless-shock measurements in homologous flows" *Astrophys. J.*, **749**, 171 (2012)